

1 Pharmacodynamics of Voriconazole for Invasive Pulmonary  
2 Scedosporiosis

3 <sup>1</sup>\*Helen Box, <sup>1</sup>\*Clara Negri, <sup>1</sup>Joanne Livermore, <sup>1</sup>Sarah Whalley, <sup>1</sup>Adam Johnson, <sup>1</sup>Laura  
4 McEntee, <sup>2</sup>Ana Alastruey-Izquierdo, <sup>3</sup>Jacques F. Meis, <sup>4</sup>Christopher Thornton, <sup>1</sup>William Hope

5 <sup>1</sup>Antimicrobial Pharmacodynamics and Therapeutics, Department of Molecular and Clinical  
6 Pharmacology, Institute of Translational Medicine, University of Liverpool

7 <sup>2</sup>Ana Alastruey-Izquierdo, Mycology Reference Laboratory, National Centre for Microbiology,  
8 Instituto de Salud Carlos III, Madrid, Spain;

9 <sup>3</sup>Department of Medical Microbiology and Infectious Diseases, Canisius-Wilhelmina Hospital  
10 and Centre of Expertise in Mycology Radboudumc/Canisius-Wilhelmina Hospital, Nijmegen,  
11 The Netherlands

12 <sup>4</sup>Biosciences, University of Exeter, Exeter, United Kingdom

13

14 Corresponding Author:

15 Professor William Hope

16 Sherrington Building

17 University of Liverpool

18 Ashton Rd.

19 Liverpool, L69 3GE

20 Phone: +44 (0)151 794 5941

21 Email: william.hope@liverpool.ac.uk

22

23 \*HB and CN made equal contributions to this work

24

25 Funding: this work was supported, in part, by the European Society for Clinical Microbiology  
26 and Infectious Diseases (ESCMID)

27

28

29

30

31 Potential conflicts of Interest

32 William Hope holds or has recently held research grants with F2G, AiCuris, Astellas Pharma,  
33 Spero Therapeutics, Matinas Biosciences, Antabio, Amplyx, Allecra, Auspherix and Pfizer. He  
34 holds awards from the National Institutes of Health, Medical Research Council, National  
35 Institute of Health Research, and the European Commission (FP7 and IMI). William Hope has  
36 received personal fees in his capacity as a consultant for F2G, Amplyx, Ausperix, Spero  
37 Therapeutics, Medicines Company, Gilead and Basilea. WH is Medical Guideline Director for  
38 the European Society of Clinical Microbiology and Infectious Diseases, and an Ordinary  
39 Council Member for the British Society of Antimicrobial Chemotherapy.

40 Ana Alastruey-Izquierdo has received grants from F2G, Scynexis, Gilead and Fondo de  
41 Investigacion Sanitaria (FIS PI13/02145) outside the submitted work.

42 J. F. M. has received grants from Astellas, Basilea, F2G and Merck; has been a consultant to  
43 Astellas, Basilea, Scynexis and Merck; and has received speaker's fees from Astellas, Merck,  
44 United Medical, Teva and Gilead.

45

46 Acknowledgment:

47 The authors acknowledge that this work was initially facilitated by an award from the  
48 European Society for Clinical Microbiology and Infectious Diseases to Dr Susan Howard.

49

## 50 ABSTRACT

51 *Scedosporium apiospermum* is a medically important fungal pathogen that causes a wide  
52 range of infections in humans. There are relatively few antifungal agents that are active  
53 against *Scedosporium* spp. Little is known about the pharmacodynamics of voriconazole  
54 against *Scedosporium*. Both static and dynamic *in vitro* models of invasive scedosporiosis  
55 were developed. Monoclonal antibodies that target a soluble cell wall antigen secreted by  
56 *Scedosporium apiospermum* were used to describe the pharmacodynamics of voriconazole.  
57 Mathematical pharmacokinetic-pharmacodynamic models were fitted to the data to estimate  
58 the drug exposure required to suppress the release of fungal antigen. The experimental  
59 results were bridged to humans using Monte Carlo simulation. All 3 strains of *S.*  
60 *apiospermum* tested invaded through the cellular bilayer of the *in vitro* models and liberated  
61 antigen. There was a concentration-dependent decline in antigen with near maximal  
62 antifungal activity in all 3 strains with 10 mg/L. Similarly, there was a drug exposure  
63 dependent decline in circulating antigen in the dynamic model and complete suppression of  
64 antigen with an AUC of approximately 80 mg.h/L. A regression of the AUC:MIC versus area  
65 under the antigen time curve showed that near maximal effect was obtained with AUC:MIC  
66 of approximately 100. Monte Carlo simulation suggested that only isolates with an MIC of  
67 0.5 mg/L enable pharmacodynamic targets to be achieved with a standard regimen of  
68 voriconazole. Isolates with higher MICs may need higher drug exposure targets than are  
69 currently recommended for other fungi.

70  
71  
72  
73  
74

75

## 76 INTRODUCTION

77 *Scedosporium* spp. are environmentally ubiquitous hyaline moulds (1). *Scedosporium*  
78 *apiospermum* is a medically important member of the *Scedosporium* genus that also  
79 comprises *Scedosporium boydii*, *Scedosporium angustum*, *Scedosporium minutisporum*,  
80 *Scedosporium dehoogii*, and *Scedosporium aurantiacum* (2, 3). Infections caused by these  
81 pathogens occur in a range of contexts that include near-drowning, solid organ  
82 transplantation, chronic lung disease (e.g. cystic fibrosis) and otherwise seemingly  
83 immunocompetent hosts (1). *Scedosporium* spp. cause diseases that are as disparate as  
84 mycetoma, airway colonisation in cystic fibrosis, pneumonia, skin and soft tissue infection  
85 and disseminated infection (4). The fungus is neurotropic and central nervous system  
86 infection has been demonstrated in experimental models of infection, and is apparent from a  
87 multitude of case studies and series (5–9).

88 Voriconazole is considered a first-line agent for the treatment of invasive infections  
89 caused by *Scedosporium apiospermum* (10). The overall treatment response for infections  
90 caused by *Scedosporium* spp. is approximately 43% (11). This disappointingly low figure  
91 raises several issues. The first is uncertainty surrounding the optimal use of voriconazole for  
92 *Scedosporium* spp. There is no specific information for this indication that informs the  
93 optimal regimen, targets for therapeutic drug monitoring or *in vitro* susceptibility  
94 breakpoints. The second is the paucity of antifungal agents that are effective for  
95 *Scedosporium* spp. The advent of newer triazoles such as posaconazole and isavuconazole do  
96 not appear to offer a significant therapeutic advance over voriconazole for the treatment of  
97 these fungi. There are no experimental pharmacodynamic models of invasive scedosporiosis  
98 that enable current antifungal agents to be optimised or newer antifungal agents to be  
99 developed.

100 Here, we adapt an existing *in vitro* cell culture model of the human alveolus that has  
101 been used for *Aspergillus fumigatus* (12) and *Aspergillus flavus* (13) infections to develop a  
102 new model of invasive pulmonary scedosporiosis. The key step in the development of the  
103 model described in this study was the use of a double- sandwich monoclonal antibody (mAb)-  
104 based ELISA for the quantification of a soluble cell wall antigen shown previously to be an  
105 accurate biomarker for tracking species in the *Scedosporium apiospermum* complex (14). The  
106 antigen provided a continuous assessment of the interaction of voriconazole with its fungal  
107 target potentially in the same way as galactomannan has been used for *Aspergillus* spp. A  
108 deep understanding of the pharmacodynamics of voriconazole against *Scedosporium* enables  
109 the design of optimised treatment regimens and is fundamental to establishing *in vitro*  
110 susceptibility breakpoints.

111

## 112 RESULTS

113 *Provenance, Identification and In Vitro Susceptibility Testing*

114 Two strains were obtained from the Spanish Mycology Reference Laboratory and a  
115 further strain from the Regional Mycology Laboratory, University Hospital, South Manchester  
116 (Table 1). No details were available as to the relevant clinical details. The three isolates used  
117 in this study were identified as *Scedosporium apiospermum* based on sequencing of the ITS  
118 and  $\beta$ -tubulin genes and searching within the FUNCBS.txt database. The MICs using Clinical  
119 Laboratory Sciences Institute (CLSI) methodology are shown in Table 1. Strains with  
120 voriconazole MICs of 0.5-1 mg/L were used for experiments so as to study isolates largely  
121 representative of a susceptible population according to MIC<sub>90</sub> values (21).

122

123 *Static models of the human alveolus*

124 A previously described cellular bilayer model of the human alveolus (15) was used to  
125 study the pharmacodynamics of voriconazole against *Scedosporium apiospermum*. The  
126 bilayer is comprised of a layer of human pulmonary arterial endothelial cells and human  
127 alveolar epithelial cells. The bilayer delineates an airspace (alveolar compartment) and blood  
128 space (endothelial compartment). Previous studies of *Aspergillus* spp. have used  
129 galactomannan as a biomarker to assess fungal invasion through the cellular bilayer and  
130 quantify the response to antifungal therapy (12, 15). In the current study, a novel cell wall  
131 antigen liberated by *Scedosporium* spp. during growth was used (see below) for this purpose.

132 Following inoculation of macroconidia into the alveolar compartment and subsequent  
133 germination, there was progressive liberation of antigen in the endothelial compartment  
134 (Figure 1). Antigen appeared in the endothelial compartment approximately 24 hours after  
135 inoculation and plateaued thereafter.

136 The exposure-response relationships for voriconazole in the static model of invasive  
137 pulmonary scedosporiosis are shown in Figure 2. In these experiments, voriconazole was  
138 administered to the endothelial compartment 6-hours post inoculation from where it  
139 distributed into the cellular bilayer and into the alveolar compartment. There was more  
140 pharmacodynamic variability in the alveolar compartment than the endothelial compartment  
141 as evidenced by the larger standard deviation of the experimental replicates. Some of the  
142 exposure response relationships in the alveolar compartment were right-shifted with respect  
143 to those in the endothelial compartment. This was apparent from the data and the estimates  
144 of EC<sub>50</sub> from the inhibitory sigmoid Emax relationship. Maximal antifungal activity, as  
145 estimated using the release of antigen, was achieved in both the alveolar and endothelial  
146 compartments of all strains with voriconazole concentrations of approximately 10 mg/L  
147 (Figure 2). Nevertheless, there was significant strain-to-strain variability in the  
148 pharmacodynamics of voriconazole.

149

150 ***Dynamic models of the human alveolus***

151 A dynamic model of invasive pulmonary scedosporiosis was developed to enable the  
152 pharmacodynamics in response to human-like pharmacokinetic profiles of voriconazole to be  
153 examined. Purpose-built bioreactors have previously been described as has the circuitry that  
154 enables the simulation of human-like pharmacokinetics (12). Samples to estimate the  
155 pharmacokinetics and pharmacodynamics of voriconazole were taken from medium passing  
156 through the endothelial compartment of the dynamic in vitro model.

157 In untreated circuits, there was a progressive increase in antigen concentrations  
158 through the experimental period. A human-like PK profile of voriconazole was simulated in  
159 the dynamic model with average  $AUC_{72-96}$  that ranged from 7.84-80.68 mg.h/L. These drug  
160 exposures were based on preliminary experiments, prior knowledge of the  
161 pharmacodynamics of voriconazole against filamentous fungi, and were also designed to  
162 encompass the entire exposure-response relationship for *Scedosporium apiospermum*.

163 There was a drug-exposure-dependent decline in antigen concentrations. As the AUC  
164 increased, there was progressively larger suppression of circulating antigen concentrations  
165 (Figure 3). An  $AUC_{0-24}$  of approximately 80 mg.h/L resulted in complete suppression of  
166 antigen release from all three strains (Figure 3). There was no evidence of a paradoxical  
167 effect with even higher drug exposures (data not shown).

168

169 ***Mathematical modelling***

170 A linked pharmacokinetic-pharmacodynamic mathematical model was fitted to the  
171 entire experimental dataset using the population pharmacokinetic program Pmetrics (16).  
172 The mathematical model fitted the PK-PD data well (Figure 4). The median parameter values  
173 fitted the data better than the means and are shown in Table 2. The Bayesian estimates for  
174 each arm (circuit) were used to calculate the area under the voriconazole concentration-time  
175 curve for each regimen from 72 to 96 hours post initiation of voriconazole using the  
176 trapezoidal rule. Similarly, the area under the antigen-time curve was estimated from the  
177 time of treatment initiation (i.e. time =0) to 96 hours post initiation of voriconazole using the  
178 Bayesian posterior estimates of each circuit and the trapezoidal rule.

179

180 ***Pharmacodynamics of voriconazole***

181 The estimates for both the voriconazole  $AUC_{72-96}$  and  $AUC_{72-96}:MIC$  versus the area  
182 under the antigen-time curve were used to establish pharmacodynamic relationships for  
183 voriconazole against *Scedosporium apiospermum*. Inhibitory sigmoid  $E_{max}$  models fitted to  
184 the data suggested that an AUC and AUC:MIC of 16.69 mg\*h/L and 22.88, respectively was

185 associated with half-maximal effect (Figure 5). The shape and coefficient of determination  
186 for the two regressions were similar, but the AUC:MIC versus effect relationship was slightly  
187 right-shifted.

188

### 189 *Bridging to Humans*

190 A standard licenced regimen was used for the simulation (i.e. 6 mg/kg i.v. q12h for  
191 two dosages followed by 4 mg/kg q12h i.v.). Voriconazole was infused over 1 hour. The  
192  $AUC_{0-24}$  at the end of 5 days of therapy was calculated using integration. Each simulated  
193 patient's AUC was divided by the MIC to calculate AUC:MIC for each MIC value. The  
194 proportion of simulated patients achieving (or exceeding) the pharmacodynamic target at  
195 each MIC was determined. The expectation of overall target attainment across the  
196 population was 34%.

197

198

## 199 DISCUSSION

200 There is only limited information on the MIC distribution of *Scedosporium*  
201 *apiospermum*. MICs estimated using Clinical Laboratory Sciences Institute (CLSI) M-38A  
202 methodology suggests that the MIC<sub>50</sub> and MIC<sub>90</sub> is 1 and 2 mg/L, respectively (17). Inspection  
203 of the MIC distribution of strains described in this study suggests that the epidemiological  
204 cut-off value for voriconazole is 4 mg/L. Using an AUC:MIC pharmacodynamic target of 100  
205 (that is associated with complete suppression of circulating antigen in the *in vitro* cell culture  
206 model) the currently licenced regimen of voriconazole (i.e. 6 mg/kg q12h for two dosages  
207 followed by 4 mg/kg q12h) has an overall probability of target attainment of 34% (i.e. 34% of  
208 simulated patients are predicted to have complete suppression of the circulating antigen  
209 when assessed against a distribution of MICs). These simulations provide experimental  
210 support a breakpoint of 0.5 mg/L, which is less than the epidemiological cutoff value of 4  
211 mg/L. These conclusions are based upon an AUC:MIC target of 100, which needs further  
212 validation using further experimental and clinical data.

213 Immunosuppressed murine models of disseminated infection of *Scedosporium* spp.  
214 have been developed and used to assess pathogenesis and efficacy of various antifungal  
215 agents. The primary model readouts include survival, and the fungal burden in kidneys,  
216 spleen, brain, liver and lungs. Infection is initiated by i.v. injection of conidia, rather than the  
217 usual clinically relevant route of infection (i.e. inhalation of conidia) (5, 18, 19). Disseminated  
218 models of fungal infection may not be ideal to establish pharmacodynamic relationships  
219 because they are not faithful mimics of human pathogenesis and disease. The model  
220 endpoints are also a potential issue. For example, survival in mice is confounded by mixing  
221 efficacy and drug-related toxicity. There are also well-established problems in performing  
222 quantitative counts from tissue homogenates to assess the fungal burden of moulds (see, for  
223 example, (20)). These limitations are further compounded by the complex pharmacology of  
224 many antifungal agents. For example, voriconazole is notoriously difficult to study in mice  
225 because of auto-induction of clearance, and a pharmacokinetic profile that is significantly  
226 different from humans (21). Hence, alternative model systems of invasive scedosporiosis are  
227 required to assess the pharmacodynamics of new and existing antifungal agents.

228 We have previously developed static and dynamic models of the human alveolus to  
229 describe the pharmacodynamics of voriconazole against *Aspergillus* spp. Outputs from these  
230 models have aligned well with the available data from laboratory animal models and clinical  
231 datasets (12, 13, 15). This has motivated the development of newer models for other  
232 medically important fungi. The use of galactomannan as a biomarker circumvents the  
233 problems in directly quantifying the burden of *Aspergillus* in tissue beds, and enables direct *in*  
234 *vivo*-to-clinical correlations. Galactomannan cannot however be used for fungi other than  
235 *Aspergillus* spp. For the *Scedosporium* studies described here, we used previously  
236 characterised monoclonal antibodies (HG12 and GA3), raised against a cell wall antigen  
237 present in species within the *Scedosporium apiospermum* complex, to determine *S.*  
238 *apiospermum* growth. The absolute identity of the antigen bound by the mAbs has yet to be

239 determined, but they bind to a carbohydrate epitope on a major 120 kDa glycoprotein  
240 secreted during active growth of *Scedosporium* spp. (14). Upon germination of conidia, the  
241 antigen ceases to be expressed on the spore surface and is then produced extracellularly by  
242 developing hyphae (14). The antigen is therefore a potentially useful biomarker for  
243 determining active growth of *Scedosporium* spp., and for tracking response to antifungal  
244 drugs.

245         The often-suboptimal clinical outcomes of patients infected with *Scedosporium*  
246 *apiospermum* complex provides the impetus to develop new antifungal agents. The  
247 availability of a range of pharmacodynamic models enables the acquisition of the  
248 underpinning evidence for patients to be enrolled in clinical trials. While there is a general  
249 paucity of compounds in development pipelines, several new compounds demonstrate *in*  
250 *vitro* activity against *Scedosporium*. These compounds include F901318 (F2G, Eccles, UK) and  
251 APX001 (Amplyx, San Diego, USA). These compounds could be further assessed in this  
252 model.

253         There are several limitations of this study. Firstly, this is a cell culture model that is  
254 representative of relatively early invasive pulmonary disease. The pharmacodynamics of  
255 voriconazole may change in later phases of established disease where there is significant  
256 tissue necrosis. Furthermore, the pharmacodynamic relationships specifically pertain to  
257 invasive pulmonary infection and may not necessarily represent other forms of infection and  
258 disease caused by *Scedosporium* spp., such as those that involve the central nervous system.  
259 The *in vitro* model does not contain immunological effectors and does not enable their  
260 adjunctive antifungal effect to be estimated. This may lead to an overestimate of the  
261 pharmacodynamic target for immunocompetent patient populations. A novel antigen was  
262 used as a biomarker to assess the pharmacodynamics of voriconazole in this experimental  
263 model. The clinical relevance of this antigen remains to be determined. This will require a  
264 combination of experimental and clinical research in the same manner as occurred for  
265 galactomannan.

266         Despite potential limitations, this *in vitro* model provides new insights into the  
267 pharmacodynamics of voriconazole against a less common, but nevertheless medically  
268 important fungal pathogen. The development of new agents and therapeutic approaches will  
269 require an array of experimental models that allow their pharmacodynamics to be elucidated  
270 and optimised. The approach of using novel soluble cell wall antigens as biomarkers with  
271 prognostic value provides a way in which the pharmacodynamics of relatively uncommon  
272 pathogens and antifungal compounds with challenging pharmacological properties can be  
273 elucidated.

274

275

276

277 **METHODS**278 ***Identification of Isolates to Species Level***

279 Isolates of *Scedosporium apiospermum* were obtained from the Regional Mycology  
280 Reference Laboratory, University Hospital of South Manchester and the Mycology Reference  
281 Laboratory, National Centre for Microbiology, Instituto de Salud Carlos III, Madrid, Spain.  
282 Isolates were stored at -80°C.

283 *Scedosporium apiospermum* was definitively identified via sequencing of the internal  
284 transcribed spacer (ITS) and  $\beta$ -tubulin regions. Extraction of fungal DNA was performed as  
285 follows. Approximately 20-40 acid-washed glass beads were suspended in 0.5 mL of sterile  
286 distilled water. The strains were grown on oatmeal agar for five days prior to  
287 experimentation. Mycelia and conidia were harvested by gently abrading the fungus with a  
288 sterile needle before adding to the beads and water. Samples were homogenised using a  
289 FastPrep-24 homogeniser. Filters (2 mm diameter) were cut from Whatman Flinders  
290 Technology Associates classic indicator cards (Whatman International, Kent, United Kingdom)  
291 and inoculated with 2  $\mu$ L of homogenate. Filters were dried for 10 minutes before being  
292 washed twice with 100  $\mu$ L sterile distilled water.

293 For the amplification of DNA, 700  $\mu$ L of polymerase chain reaction (PCR) reaction mix  
294 was prepared. This consisted of 70  $\mu$ L buffer (QIAGEN, UK), 7  $\mu$ L dNTPs (2.5mM), 70  $\mu$ L  
295 forward primer, 70  $\mu$ L reverse primers, 420  $\mu$ L PCR grade H<sub>2</sub>O, 3.5  $\mu$ L HotstarTaq (QIAGEN,  
296 UK). The PCR reaction mixture was vortexed for 1 min. A total of 100  $\mu$ L of PCR reaction  
297 mixture was added to each PCR tube containing the inoculated filter. The PCR reaction  
298 conditions were as follows: 15mins 94°C for one cycle, 40 cycles of 30 sec at 94°C, 30 sec  
299 50°C, 90 sec 72°C, one cycle of 7 mins at 72°C, 4°C for remainder. After the PCR cycle was  
300 completed, 8  $\mu$ L was transferred to a new PCR tube and 5  $\mu$ L of the appropriate forward  
301 primer was added for sequencing of the ITS and  $\beta$ -tubulin regions.

302 Sequencing of the amplicons was performed by Beckman- Coulter Genomics Inc.  
303 Sequences were analysed for identification via the FUNCBS.txt database  
304 (<http://www.cbs.knaw.nl/Collections/BioloMICSSequences.aspx>).

305

306 ***Preparation of Inoculum for Experimental Pharmacology***

307 Ten days prior to experimentation, isolates were sub-cultured to oatmeal agar  
308 (Sigma-Aldrich, Poole, UK) and incubated in air at 30°C. Conidial suspensions were prepared  
309 by flooding a flask with 20 mL of PBS and simultaneously abrading the surface of the colonies  
310 with a sterile cotton swab. The resulting suspension was filtered through sterile gauze before  
311 being centrifuged for 10 minutes at 2500 rpm and re-suspending the pellet in 10mL PBS. The  
312 washing step was performed twice. For the preparation of the final inoculum, basal cell

313 culture medium, EBM-2, (Promocell, Heidelberg, Germany) was used as the diluent. A conidial  
314 suspension of  $1 \times 10^6$  CFU/mL was prepared using a haemocytometer and confirmed by  
315 quantitative cultures by plating to Sabouraud agar supplemented with chloramphenicol  
316 (Oxoid Ltd, Basingstoke, UK).

317

### 318 *In vitro Susceptibility Testing*

319 Minimum inhibitory concentrations (MIC) of voriconazole against *S. apiospermum*  
320 isolates were determined in five independently conducted experiments using Clinical  
321 Laboratory Sciences Institute (CLSI) methodology.

322

### 323 *Cell Culture Models of Invasive Scedosporiosis*

324 Novel cell culture models of invasive pulmonary scedosporiosis were developed to  
325 investigate the pharmacodynamics of voriconazole. These were based on similar models  
326 developed for *Aspergillus fumigatus* and *Aspergillus flavus* (12, 13, 15). Both static and  
327 dynamic models of invasive disease were developed. In the former, drug concentrations were  
328 fixed, as occurs in *in vitro* susceptibility testing. In the latter, peristaltic pumps were used to  
329 simulate human pharmacokinetics to ensure a more clinically relevant and tractable estimate  
330 of drug exposure.

331 Both model systems required the construction of a cellular bilayer consisting of  
332 human pulmonary arterial endothelial cells (HPAECs) (Promocell, Heidelberg, Germany) and  
333 human alveolar epithelial cells (A549s; LGC Standards, Middlesex, UK). Cells were seeded on  
334 opposing surfaces of polyester membrane cell culture inserts, as previously described (15).

335

### 336 *Growth of A549 and HPAECs cells*

337 A549 cells were cultured using endothelial basal medium-2 (EBM-2; Invitrogen,  
338 Paisley, UK) medium containing 10% foetal bovine serum (FBS). HPAECs were cultured using  
339 endothelial growth medium (EGM-2) according to the manufacturer's instructions  
340 (Promocell, Heidelberg, Germany), which consists of EBM-2 supplemented with 2% FBS  
341 (Invitrogen, Paisley, UK), ascorbic acid, heparin, hydrocortisone, human endothelial growth  
342 factor, vascular endothelial growth factor 165, human fibroblast factor B and R-3-insulinlike  
343 growth factor 1.

344 Once 70-80% confluence was achieved, cells were washed using Hanks Balanced Salt  
345 Solution (HBSS) (Sigma-Aldrich, Poole, UK) and harvested with 6 mL of a 0.25% trypsin-  
346 ethylenediaminetetraacetic (EDTA) solution (Sigma-Aldrich, Poole, UK). Cells were then  
347 centrifuged for 5 min. at 2,000 rpm and re-suspended in the appropriate medium to achieve  
348 final density of  $5.5 \times 10^5$ /mL and  $1 \times 10^6$ /mL for A549s and HPAECs, respectively.

349

350 ***Construction of the Static Model of Invasive Pulmonary Scedosporiosis***

351 12 mm cell culture inserts with a 3.0  $\mu\text{m}$  pore polyester membrane for 24-well tissue  
352 culture plates (Appleton Woods, Birmingham, UK) were inverted. For the construction of the  
353 endothelial cell layer 100  $\mu\text{L}$  of HPEAC cell suspension was pipetted onto the underside of the  
354 membrane. Inserts were then incubated (37°C, 5%  $\text{CO}_2$ ) for 2 hours to enable cellular  
355 adhesion to the membrane. Inserts were then transferred to 24-well plates containing 0.6 mL  
356 of EGM-2 medium. One-hundred  $\mu\text{L}$  of EBM-2 containing 10% FBS was then added to the  
357 alveolar compartment. The cell culture plates were then incubated at 37°C in 5%  $\text{CO}_2$  for 24  
358 hours.

359 After 24 hours, medium from the alveolar compartments was removed and inserts  
360 were transferred to new plates containing the relevant amounts of fresh EGM-2 medium.  
361 One-hundred  $\mu\text{L}$  of the A549 suspension was added to the alveolar compartment. After 2  
362 hours, medium from the alveolar compartment was removed to create an air-liquid interface.  
363 The EGM-2 medium in the bottom compartment was replaced every 48 hours and medium  
364 that had accumulated in the alveolar compartments was removed and discarded. The  
365 bilayers were ready for experimentation after 5 days.

366

367 ***Construction of the Dynamic Model of Invasive Pulmonary Scedosporiosis***

368 The same process was used for the dynamic models except larger 12-well cell culture  
369 plate inserts were used (Greiner Bio-One, Stonehouse, UK). Larger volumes were required  
370 because of the larger surface areas, hence, 400  $\mu\text{L}$  of the HPAEC suspension, and 400  $\mu\text{L}$  of the  
371 A549 suspension was used to seed the membrane. Inserts were immersed in 1.5 mL of EGM-2  
372 medium in 12-well tissue culture plates. The protocols for establishing the bilayer were the  
373 same as for the static model.

374

375 ***Pharmacodynamic Experiments Using the Static in Vitro Model of the Human Alveolus***

376 Cell culture inserts were transferred to a 24 well plate containing 0.6 mL of EBM-2  
377 medium supplemented with 2% FBS. A conidial suspension of  $1 \times 10^6$  of *Scedosporium*  
378 *apiospermum* was prepared and warmed to 37°C for 20 minutes. One-hundred  $\mu\text{L}$  of the  
379 conidial suspension was inoculated into the alveolar compartment of each cell culture insert  
380 and incubated at 37°C in 5%  $\text{CO}_2$  for 12 hours. The remaining (spent) inoculum was then  
381 removed and discarded to enable an air-liquid interface to re-establish.

382 Pure voriconazole was dissolved in DMSO (Sigma- Aldrich, Poole) to produce a stock  
383 solution of 3 mg/ml. The desired final concentration of voriconazole for each insert was  
384 achieved by serial dilution of the stock in EBM-2 medium that was supplemented with 2%

385 FBS. Medium containing different concentrations of voriconazole was placed in each well 12  
386 hours post inoculation in order to replicate an early invasive infection. Plates were then  
387 incubated at 37°C, 5% CO<sub>2</sub> for 48 hrs. Samples from the endothelial and alveolar  
388 compartments were obtained and stored at -80°C for measurement of drug concentrations  
389 and detection of the cell wall antigen.

390

### 391 *Construction of dynamic model*

392 Cell culture inserts were housed in custom-designed stainless steel bioreactors.  
393 Bioreactors were specifically engineered to house individual cell culture inserts and allowing  
394 media to flow past the endothelial layer. All components were autoclaved and circuits were  
395 assembled in a class II safety cabinet.

396 Each bioreactor was connected to a circuit using Marprene® thermoplastic  
397 elastometer tubing (Watson Marlow, Cornwall, UK). All connections were made using  
398 polypropylene barbed luer adapters (Cole Palmer, London UK; West Group, Hants, UK). A  
399 central reservoir containing 200 mL of warmed media was connected to the circuit using 1.5-  
400 mm bore polytetrafluoroethylene (PTFE) semi-rigid tubing (Diba Labware, Kinesis Ltd.,  
401 Cambridge, UK) fitted into Omni-Fit Q-series bottle caps (Diba Labware, Kinesis Ltd.,  
402 Cambridge, UK). The central reservoir contained a magnetic stirring bar to ensure continuous  
403 mixing of drug. Duran bottles containing fresh medium and empty bottles for the removal of  
404 waste were connected to the central reservoir using Silastic®, 1.6 mm bore tubing (Dow  
405 Corning) to enable the generation of first-order decay in voriconazole concentrations. Two  
406 205-U multichannel cassette peristaltic pumps fitted with 1.52 mm bore Marprene manifold  
407 tubing (Watson Marlow, Cornwall, UK) were used to circulate medium through the circuit  
408 and bioreactor.

409 Once assembled, circuits were transferred to a 37°C incubator for the remainder of  
410 the experiment. Dulbecco's modified Eagle medium (DMEM) containing 4500 mg/L D-  
411 Glucose, L-Glutamine and HEPES buffer (Invitrogen, Paisley, UK) was supplemented with 2%  
412 FBS and a penicillin- streptomycin solution (Sigma-Aldrich, Poole) to give a final concentration  
413 of 100 U/mL penicillin and 0.1 mg/mL streptomycin.

414

### 415 *Pharmacokinetic and Pharmacodynamic Experiments Using the Dynamic in Vitro Model of the* 416 *Human Alveolus*

417 Pure voriconazole powder was dissolved in DMSO. Drug was administered directly  
418 into the central compartment as a bolus. Dosages were selected from previously published  
419 data demonstrating the achievement of voriconazole exposures that ranged from sub-  
420 optimal to successful in treating organisms of similar susceptibilities in this model (13).  
421 Amounts of 0 mg, 0.1 mg, 0.2 mg, 1 mg and 3 mg were administered every 12 hours to the

422 central compartment to achieve initial concentrations of 0, 0.5, 1.5, 5 and 15 mg/L  
423 respectively. The pump connecting the Duran containing fresh medium and the waste was  
424 run to achieve a flow of 10 mL/hour. This was previously demonstrated to generate human-  
425 like concentration- time profiles for voriconazole (13). Voriconazole therapy commenced 12  
426 hours post inoculation (as was the case with the static model described above).

#### 427 **LC/MS/MS**

428 Voriconazole concentrations were measured using a validated ultrahigh-performance  
429 liquid chromatography tandem mass spectrometry method comprising of a Agilent 6420  
430 Triple Quad Mass spectrometer and a Agilent 1290 infinity LC system (Agilent Technologies  
431 UK Ltd, Cheshire, UK). Voriconazole was extracted by protein precipitation; 300 µl of  
432 acetonitrile containing the internal standard (IS) Phenacetin 0.1 mg/L (Sigma Aldrich, Dorset,  
433 UK) was added to 100 µl of matrix. The samples were then vortexed for 5 seconds and  
434 centrifuged at 13000 g for 3 minutes. Two hundred µl of the supernatant was removed and  
435 placed in 96 well plate, 3 µl were injected on an Agilent a Zorbax Eclipse Plus C18 (2.1 by 50  
436 mm, 1.8-µm particle size) (Agilent Technologies UK Ltd, Cheshire, UK).

437 Chromatographic separation was achieved using a gradient with the starting  
438 conditions of 70:30 (0.1% formic acid in water as mobile phase A and 0.1% formic acid in  
439 acetonitrile as mobile phase B). Starting conditions were held for 0.2 minutes, then mobile  
440 phase B was increased to 100% over 1.5 minutes. This was held at 100% mobile phase B for  
441 0.5 minutes, and then reduced to starting conditions for 1 minute of equilibration. The mass  
442 spectrometer was operated in multiple reaction monitoring (MRM) scan mode in positive  
443 polarity. The precursor ion for voriconazole was 350.0m/z, and it was 180.1 m/z for the IS.  
444 The product ion for voriconazole was 281.1 m/z and it was 110.0 m/z for the IS. The source  
445 parameters were set as 4000 V for capillary voltage, 350°C for gas temperature, and 60 lb/in<sup>2</sup>  
446 for the nebulizer gas. The standard curve for voriconazole encompassed the concentration  
447 range of 0.025-20.0 mg/L and was constructed using blank matrix. The data were acquired  
448 and processed using the Mass Hunter Quantitation B.6.0 software package. For voriconazole  
449 in media the limit of detection was 0.0025 mg/L and the limit of quantitation was 0.0025  
450 mg/L. The CV% was 8.9% over the concentration range 0.0025-20.0 mg/L and the intra and  
451 inter-day variation was < 7.2%.

452

#### 453 **Enzyme linked immunosorbent assay**

454 Elucidation of the pharmacodynamics of voriconazole against *S. apiospermum* was  
455 enabled by measuring a soluble cell wall antigen released during active growth of the  
456 pathogen using a double-antibody-sandwich (DAS)-ELISA. The HG12 and GA3 monoclonal  
457 antibodies used in the DAS-ELISA are specific to *Scedosporium* spp., and bind to an  
458 extracellular 120-kDa antigen secreted by hyphae following spore germination (14). Fifty µL  
459 volumes of mAb HG12 (IgG1) tissue culture supernatant (TCS) were used to coat the wells of

460 Maxisorp microtiter plates (Fisher Scientific, Loughborough, UK). The plates were incubated  
461 for 16 hours at 4°C before washing four times with PBS containing 0.05% (v/v) Tween 20  
462 (PBST). The plates were then washed once with PBS and once with distilled water before  
463 being placed in a drying cabinet at 23°C for 1 hour. Plates were stored at 4°C in sealed plastic  
464 bags until used.

465 Working volumes were 50 µL; all incubation steps were conducted in sealed plastic  
466 bags at 23°C, and wells were washed three times with PBST (5 minutes each time) between  
467 incubations. Wells containing immobilised HG12 were blocked for 10 minutes with 100µL of  
468 PBS containing 1% (w/v) of bovine serum albumin (BSA) to prevent non-specific protein  
469 binding. Blocked wells were then incubated with experimental solutions for 2 hours to allow  
470 antigen capture by mAb HG12. Unbound antigen was removed by washing with PSBT and the  
471 wells then incubated with mAb GA3 (IgM) TCS for 1 hour. Washed wells were then incubated  
472 for 1 hour with goat anti-mouse IgM (µ-chain specific) biotin conjugate (Sigma Aldrich, Poole,  
473 UK) diluted 1:1000 in PBST containing 0.5% (w/v) BSA. After removal of unbound biotin  
474 conjugate by washing with PBST, wells were incubated for a further hour with Extravidin-  
475 peroxidase (Sigma-Aldrich, Poole, UK) diluted 1:1000 in PBST containing 0.5% (w/v) BSA. After  
476 washing with PBST and a single rinse with PBS, bound antibody-antigen complexes were  
477 visualized by incubating wells in tetramethyl benzidine (TMB) substrate solution (Sigma-  
478 Aldrich, Poole, UK) for 30 minutes. Reactions were stopped by the addition of 3M H<sub>2</sub>SO<sub>4</sub> and  
479 absorbance values determined at 450 nm.

#### 480 **Mathematical Modelling**

481 A population methodology was used to fit a mathematical model to the data from  
482 each isolate. For *Scedosporium* datasets the structural mathematical model consisted of the  
483 following two inhomogeneous ordinary differential equations:

484

$$485 \quad dX1/dt= B(1)-(SCL/V)*X1 \quad \text{Equation 1}$$

$$486 \quad dN/dt=Kgmax*(1-(N/POPMAX))*N \quad \text{Equation 2a}$$

$$487 \quad *(1-(X1/Vc)^{Hg}/(X1/Vc)^{Hg}+C50g^{Hg}) \quad \text{Equation 2b}$$

488

489 with output equations

$$490 \quad Y(1)=X(1)/V \quad \text{Equation 3}$$

$$491 \quad Y(2)=X(2) \quad \text{Equation 4}$$

492

493 Where: B(1) represents a bolus input of voriconazole into the central compartment, SCL is  
494 the clearance of drug from the circuit, Vc is the volume of the circuit, N is the antigen value,

495 Kgmax is the maximal rate of growth; POPMAX is the theoretical maximal antigen  
496 concentration within the circuit; Hg is the slope function for the suppression of growth; and,  
497 C<sub>50g</sub> is the concentration of drug in the circuit where there is half-maximal suppression of  
498 growth.

499 Equation 1 describes the rate of change of the mass of voriconazole in the circuit. Equation 2  
500 describes the rate of change of antigen in the circuit and contains terms that describe fungal  
501 growth in the absence of drug (Equation 2a) and the drug induced suppression of growth  
502 (Equation 2b).

503

#### 504 ***Pharmacodynamic Target Associated with Maximal Antifungal Activity***

505 The mathematical model fitted to each strain was used to estimate the voriconazole  
506 area under the concentration-time curve and the area under the antigen-time curve. Each  
507 circuit contributed one summary estimate of the effect of voriconazole.

508 The relationship between drug exposure and the effect on the biomarker was  
509 modelled using an inhibitory sigmoid Emax function that took the form:

$$510 \text{ Effect} = E_{con} - \frac{E_{max} * \text{Drug Exposure}^H}{EC_{50}^H + \text{Drug Exposure}^H}$$

511 Where: E<sub>con</sub> is the antigen in controls, E<sub>max</sub> is the maximum antifungal effect induced by  
512 voriconazole, Drug exposure is the AUC or AUC:MIC of voriconazole, H is the slope (Hill)  
513 function and EC<sub>50</sub> is the voriconazole drug exposure where the effect is half maximal. The  
514 model was fitted to the data using the pharmacokinetic program ADAPT5.

515

#### 516 ***Monte Carlo Simulation and Bridging Studies***

517 Monte Carlo simulations were performed in ADAPT 5 (22) using a previously  
518 published population pharmacokinetic model for voriconazole (23). This model was fitted to  
519 data from healthy volunteers and patients receiving voriconazole therapy for proven or  
520 probable invasive aspergillosis. The mean parameter values and their associated variances  
521 were used and embedded in subroutine PRIOR of ADAPT 5. A log normal distribution was  
522 used and the ability of the simulation to reproduce the original parameter estimates and  
523 their dispersions was assessed. A standard licenced regimen was used for the simulation (i.e.  
524 6 mg/kg i.v. q12h for two dosages followed by 4 mg/kg q12h i.v.). Voriconazole was infused  
525 over 1 hour. The AUC<sub>0-24</sub> at the end of 5 days of therapy was calculated using integration.  
526 Each simulated patient's AUC was divided by the MIC to calculate AUC:MIC for each MIC  
527 value. The proportion of simulated patients achieving (or exceeding) the pharmacodynamic  
528 target at each MIC was determined. The MICs used for these calculations were determined  
529 using CLSI methodology and provided by Professor Jacque Meis.

## 530 REFERENCES

- 531 1. Cortez KJ, Roilides E, Quiroz-Telles F, Meletiadiis J, Antachopoulos C, Knudsen T, Buchanan W,  
532 Milanovich J, Sutton DA, Fothergill A, Rinaldi MG, Shea YR, Zaoutis T, Kottitil S, Walsh TJ.  
533 2008. Infections caused by *Scedosporium* spp. Clin Microbiol Rev 21:157–197.
- 534 2. Gilgado F, Gené J, Cano J, Guarro J. 2010. Heterothallism in *Scedosporium apiospermum* and  
535 description of its teleomorph *Pseudallescheria apiosperma* sp. nov. Med Mycol 48:122–128.
- 536 3. Gilgado F, Cano J, Gené J, Sutton DA, Guarro J. 2008. Molecular and phenotypic data  
537 supporting distinct species statuses for *Scedosporium apiospermum* and *Pseudallescheria*  
538 *boydii* and the proposed new species *Scedosporium dehoogii*. J Clin Microbiol 46:766–771.
- 539 4. Husain S, Munoz P, Forrest G, Alexander BD, Somani J, Brennan K, Wagener MM, Singh N.  
540 2005. Infections Due to *Scedosporium apiospermum* and *Scedosporium prolificans* in  
541 Transplant Recipients: Clinical Characteristics and Impact of Antifungal Agent Therapy on  
542 Outcome. Clin Infect Dis 40:89–99.
- 543 5. Capilla J, Mayayo E, Serena C, Pastor FJ, Guarro J. 2004. A novel murine model of cerebral  
544 scedosporiosis: lack of efficacy of amphotericin B. J Antimicrob Chemother 54:1092–5.
- 545 6. Lin D, Qurat-Ul-Ain K, Lai S, Musher DM, Hamill R. 2013. Cerebral *Scedosporium apiospermum*  
546 infection presenting with intestinal manifestations. Infection 41:723–726.
- 547 7. Sharma A, Singh D, A. S, Sharma A, Singh D. 2015. *Scedosporium apiospermum* causing brain  
548 abscess in a renal allograft recipient. Saudi J Kidney Dis Transpl 26:1253–1256.
- 549 8. Rodríguez MM, Pastor FJ, Salas V, Calvo E, Mayayo E, Guarro J. 2010. Experimental murine  
550 scedosporiosis: Histopathology and azole treatment. Antimicrob Agents Chemother 54:3980–  
551 3984.
- 552 9. Lelievre B, Legras P, Godon C, Franconi F, Saint-Andre JP, Bouchara J-P, Diquet B. 2013.  
553 Experimental models of disseminated scedosporiosis with cerebral involvement. J Pharmacol  
554 Exp Ther 345:198–205.
- 555 10. Tortorano AM, Richardson M, Roilides E, van Diepeningen A, Caira M, Munoz P, Johnson E,  
556 Meletiadiis J, Pana Z-D, Lackner M, Verweij P, Freiburger T, Cornely OA, Arikan-Akdagli S,  
557 Dannaoui E, Groll AH, Lagrou K, Chakrabarti A, Lanternier F, Pagano L, Skiada A, Akova M,  
558 Arendrup MC, Boekhout T, Chowdhary A, Cuenca-Estrella M, Guinea J, Guarro J, de Hoog S,  
559 Hope W, Kathuria S, Lortholary O, Meis JF, Ullmann AJ, Petrikos G, Lass-Flörl C. 2014.  
560 ESCMID and ECMM joint guidelines on diagnosis and management of hyalohyphomycosis:  
561 *Fusarium* spp., *Scedosporium* spp. and others. Clin Microbiol Infect 20.
- 562 11. Troke P, Aguirrebengoa K, Arteaga C, Ellis D, Heath CH, Lutsar I, Rovira M, Nguyen Q, Slavin  
563 M, Chen SCA. 2008. Treatment of scedosporiosis with voriconazole: Clinical experience with  
564 107 patients. Antimicrob Agents Chemother 52:1743–1750.
- 565 12. Jeans AR, Howard SJ, Al-Nakeeb Z, Goodwin J, Gregson L, Majithiya JB, Lass-Flörl C, Cuenca-  
566 Estrella M, Arendrup MC, Warn PA, Hope WW. 2012. Pharmacodynamics of voriconazole in a  
567 dynamic in vitro model of invasive pulmonary aspergillosis: Implications for in vitro  
568 susceptibility breakpoints. J Infect Dis 206:442–452.
- 569 13. Negri CE, Johnson A, McEntee L, Box H, Whalley S, Schwartz JA, Ramos-Martín V, Livermore J,  
570 Kolamunnage-Dona R, Colombo AL, Hope WW. 2017. Pharmacodynamics of the novel  
571 antifungal agent F901318 for acute sinopulmonary aspergillosis caused by *Aspergillus flavus*. J  
572 Infect Dis.

- 573 14. Thornton CR. 2009. Tracking the emerging human pathogen *Pseudallescheria boydii* by using  
574 highly specific monoclonal antibodies. Clin Vaccine Immunol 16:756–764.
- 575 15. Hope WW, Kruhlak MJ, Lyman CA, Petraitiene R, Petraitis V, Francesconi A, Kasai M, Mickiene  
576 D, Sein T, Peter J, Kelaher AM, Hughes JE, Cotton MP, Cotten CJ, Bacher J, Tripathi S,  
577 Bermudez L, Mangel TK, Zerfas PM, Wingard JR, Drusano GL, Walsh TJ. 2007. Pathogenesis of  
578 *Aspergillus fumigatus* and the kinetics of galactomannan in an in vitro model of early invasive  
579 pulmonary aspergillosis: Implications for antifungal therapy. J Infect Dis 195.
- 580 16. Neely MN, van Guilder MG, Yamada WM, Schumitzky A, Jelliffe RW. 2012. Accurate detection  
581 of outliers and subpopulations with Pmetrics, a nonparametric and parametric  
582 pharmacometric modeling and simulation package for R. Ther Drug Monit 34:467–76.
- 583 17. Lackner M, Verweij PE, Najafzadeh MJ, Curfs-breuker I, Meis JF. 2012. Species-Specific  
584 Antifungal Susceptibility Patterns of 2635–2642.
- 585 18. Gonzalez GM, Tijerina R, Najvar L, Rinaldi M, Yeh IT, Graybill JR. 2002. Experimental murine  
586 model of disseminated *Pseudallescheria* infection. Med Mycol 40:243–248.
- 587 19. Capilla J, Guarro J. 2004. Correlation between in vitro susceptibility of *Scedosporium*  
588 *apiospermum* to voriconazole and in vivo outcome of scedosporiosis in guinea pigs.  
589 Antimicrob Agents Chemother 48:4009–4011.
- 590 20. Bowman JC, Abruzzo GK, Anderson JW, Flattery AM, Gill CJ, Pikounis VB, Schmatz DM,  
591 Liberator PA, Douglas CM. 2001. Quantitative PCR Assay To Measure *Aspergillus fumigatus*  
592 Burden in a Murine Model of Disseminated Aspergillosis : Demonstration of Efficacy of  
593 Caspofungin Acetate 45:3474–3481.
- 594 21. Roffey SJ, Cole S, Comby P, Gibson D, Jezequel SG, Nedderman ANR, Smith DA, Walker DK,  
595 Wood N, Dynamics P, Metabolism SJR, C DSEP. 2003. The disposition of voriconazole in  
596 mouse, rat, rabbit, guinea pig, dog, and human. Drug Metab Dispos 2003/05/21. 31:731–741.
- 597 22. D’Argenio DZ, Schumitzky A, Wang X. 2009. ADAPT 5 User’s Guide:  
598 Pharmacokinetic/Pharmacodynamic Systems Analysis Software. Biomedical Simulations  
599 Resource, Los Angeles.
- 600 23. Hope WW. 2012. Population pharmacokinetics of voriconazole in adults. Antimicrob Agents  
601 Chemother 56:526–531.
- 602
- 603

604 Table 1. Challenge Strains of *Scedosporium apiospermum*

Strain <sup>b</sup>	Antifungal Agent <sup>a</sup>						
	AMB	ITRA	VORI	POSA	ISA	ANI	MICA
8353	16	>16	0.5	1	4	8	0.5
CNM- CM6322	8	>16	1	1	4	4	0.5
CNM- CM6386	>16	>16	1	2	8	8	8

605

606 <sup>a</sup>Strains of *Scedosporium apiospermum* used in this study and their minimum inhibitory  
607 concentrations (mg/L) determined using Clinical Laboratory Sciences Institute (CLSI)  
608 methodology. <sup>b</sup>Antifungal agents are as follows: AMB (amphotericin B), ITRA (itraconazole),  
609 VORI (voriconazole), POSA (posaconazole), ISA (isavuconazole), ANI (anidulafungin) and MICA  
610 (micafungin).

611

612

613

614

615

616

617

618

619

620

621

622

623

624

625

626

627

628 Table 2. Parameters from the pharmacokinetic-pharmacodynamic model fitted to the  
629 experimental data from each strain.

630

Parameter <sup>a</sup>	Strain 1 (8353)	Strain 2 (6322)	Strain 3 (6386)
SCL (L/h)	0.021	0.019	0.030
V (L)	0.646	0.850	1.036
Kgmax (OD <sub>450</sub> /h)	0.036	0.013	0.021
POPMAX (OD <sub>450</sub> )	1.808	2.068	2.999
C <sub>50</sub> (mg/L)	0.469	0.455	0.902
Hg	5.582	9.932	2.155
Initial Condition (OD <sub>450</sub> )	0.046	0.121	0.091

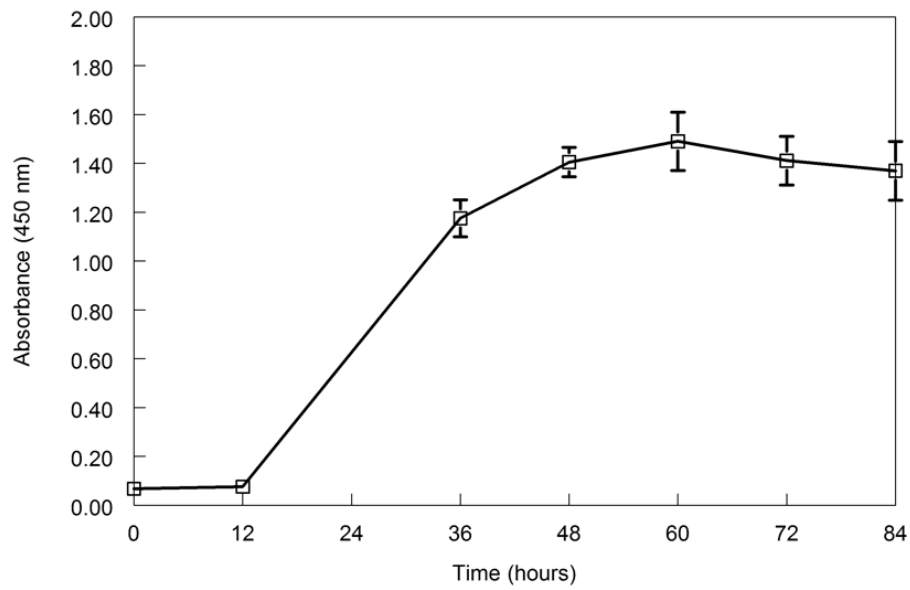
631

632 <sup>a</sup>The median parameter values are shown and are as follows: SCL (L/h) is the clearance of  
633 voriconazole from the circuit; V (L) is the volume of the central compartment; Kgmax is the  
634 maximum rate of fungal growth as estimated by the increase in fungal antigen liberated into  
635 the circuit; POPMAX is the maximum theoretical fungal density; C<sub>50</sub> is the concentration of  
636 voriconazole where there is a 50% reduction in the rate of growth; Hg is the slope function  
637 and the Initial Condition is the estimated fungal density at time of treatment initiation (which  
638 is 12 hours postinoculation).

639

640

641



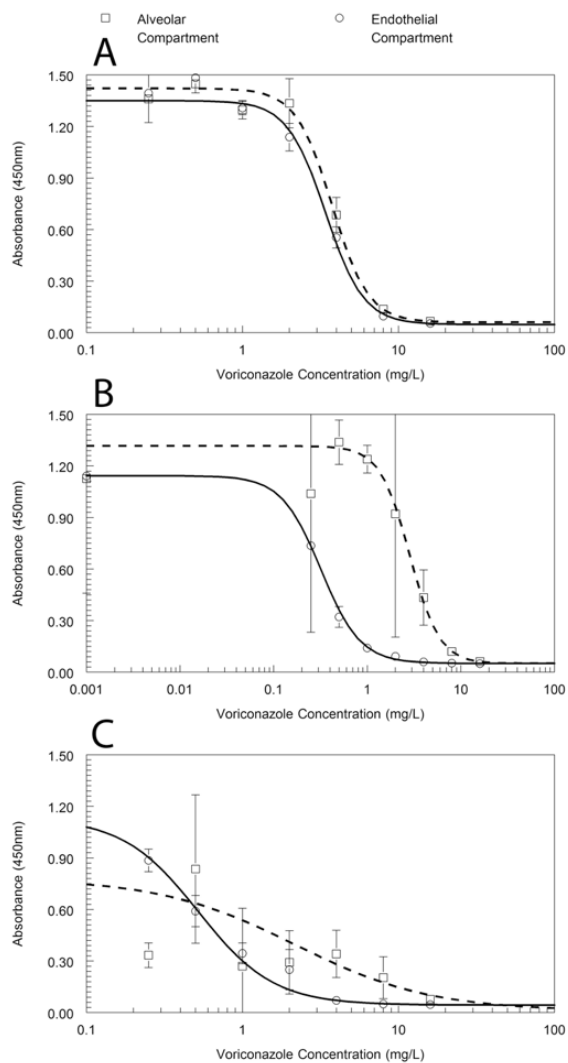
642

643 Figure 1. The time-course of antigen release in the *in vitro* static model. Data are the mean  $\pm$   
644 standard deviation of three inserts. Data were generated with strain 8353.

645

646

647



648

649

650 Figure 2. The concentration-response relationships for the three challenge strains of  
 651 *Scedosporium apiospermum*. Data are mean  $\pm$  standard deviation. The broken and solid  
 652 lines are the fit of an inhibitory sigmoid Emax model to the data from the alveolar and  
 653 endothelial compartments, respectively. Panel A, strain 8353; Panel B, 6386; Panel C 6322.

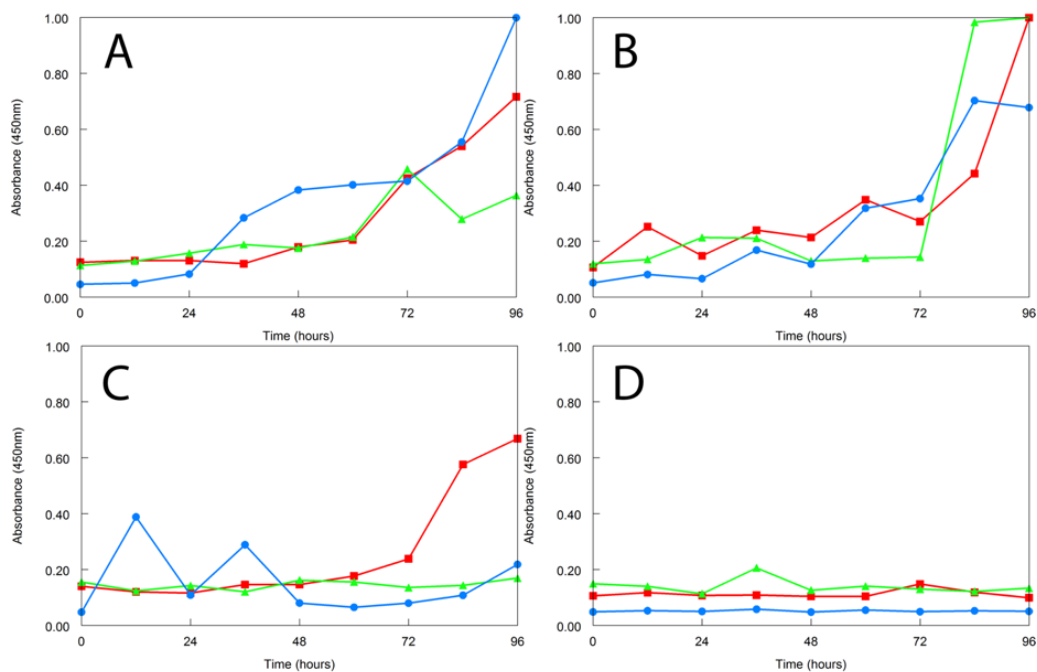
654

655

656

657

658



659

660 Figure 3. Pharmacodynamics of voriconazole against *Scedosporium apiospermum* isolates  
 661 from dynamic models of invasive pulmonary scedosporiosis. Time zero is the time of  
 662 treatment initiation and is 12 hours post inoculation. Each line represents data from a single  
 663 strain. Voriconazole was administered at time = zero and every 12 hours thereafter. Drug was  
 664 administered as a bolus. Pharmacodynamic samples were obtained from the endothelial  
 665 compartment of the model. The challenge strains are as follows: 6386 (red squares), 6322  
 666 (green triangles) and 8353 (blue circles). Panel A, Vehicle-treated control; Panel B,  
 667 average AUC = 7.84 mg.h/L inducing negligible effect; Panel C, average AUC = 15.62 mg.h/L inducing  
 668 submaximal antifungal activity, Panel D, average AUC = 80.68 mg.h/L inducing near maximal  
 669 antifungal activity.

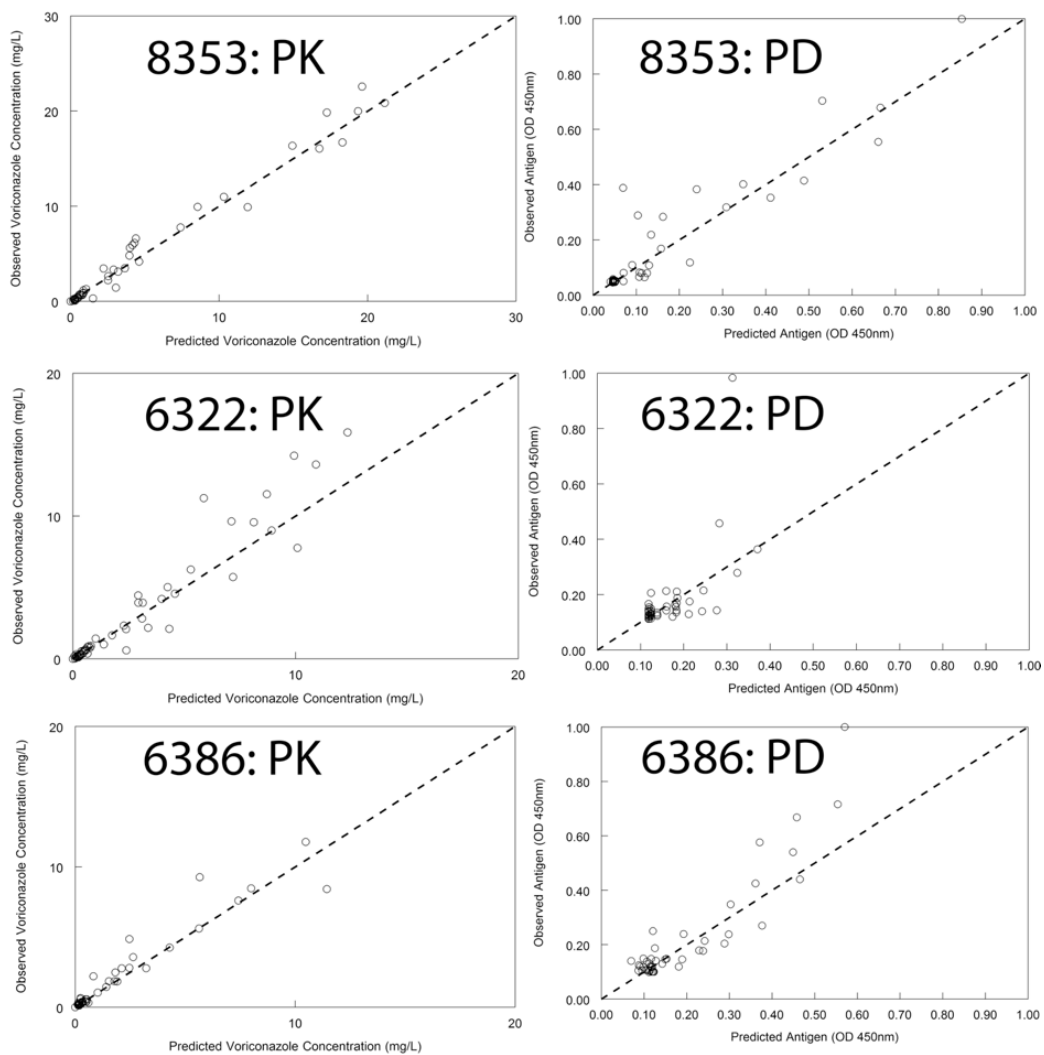
670

671

672

673

674



675

676

677

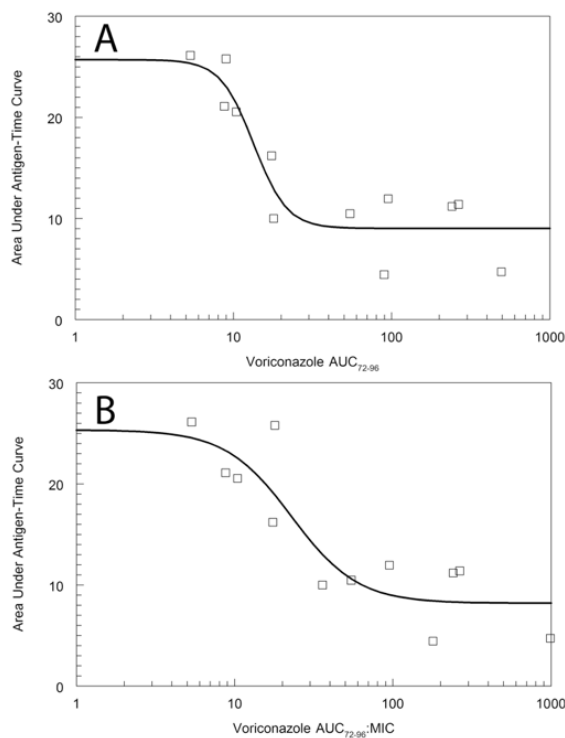
678

679

680

Figure 4. Observed-predicted values from the mathematical models fitted to the pharmacokinetic and pharmacodynamic data from each strain. The broken line is the line of identity (observed = predicted).

681



682

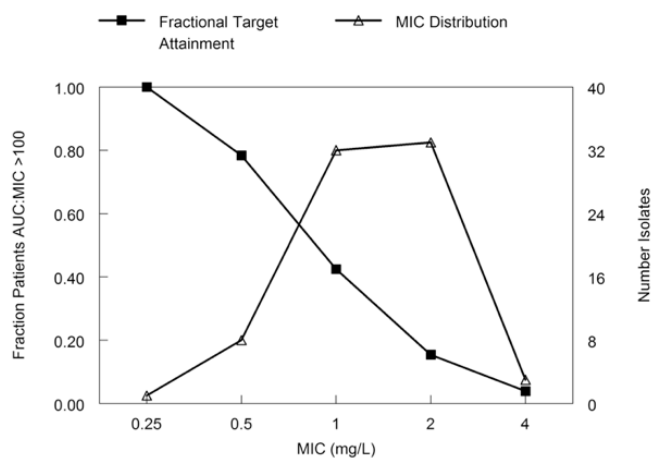
683

684 Figure 5. Panel A, The relationship between voriconazole  $AUC_{72-96}$  and the antifungal effect  
 685 quantified in terms of the area under the antigen-time curve. The inhibitory sigmoid Emax  
 686 model is given by  $\text{Area Under Antigen-Time Curve} = 25.71 -$   
 687  $(16.69 * (AUC)^{4.15} / (13.42^{4.15} + (AUC)^{4.15}))$ ;  $r^2$  0.86; Panel B, The relationship between  
 688 voriconazole  $AUC_{72-96} : MIC$  and the antifungal effect quantified in terms of the area under the  
 689 antigen-time curve. The inhibitory sigmoid Emax model is given by  $\text{Area Under Antigen-Time}$   
 690  $\text{Curve} = 25.34 - (17.14 * (AUC : MIC)^{2.09} / (22.88^{2.09} + (AUC : MIC)^{2.09}))$ ;  $r^2$  0.82.

691

692

693



694

695 Figure 6. The probability of target attainment for a regimen of i.v. voriconazole 6 mg/kg q12h  
 696 for two dosages followed by 4 mg/kg q12h thereafter. Drug was infused over 1 hour. A  
 697 weight of 75 kg was used for the simulations and the  $AUC_{0-24}$  was determined at the end of  
 698 day 5. The fraction of 5,000 simulated patients that achieved an AUC:MIC of >100 for each  
 699 MIC value is shown by the solid squares. The MIC distribution of *S. apiospermum* from 77  
 700 strains is shown by the open triangles. The overall expectation of target attainment for the  
 701 population is 34%.

702